EPR Studies on Telechelic Polymers: Characterization of Ion Multiplets

Volker Schädler, Achim Franck, Ulrich Wiesner,* and Hans W. Spiess

Max-Planck-Institut für Polymerforschung, Postfach 3148, D-55021 Mainz, Germany

Received October 28, 1996; Revised Manuscript Received April 14, 1997⊗

ABSTRACT: Endfunctionalized polyisoprenes (PI) and polystyrenes (PS) with either one sulfonate or ammonium end group and α,ω-macrozwitterionic PI and PS have been synthesized and investigated by CW-EPR using the spin probe technique. From the extrema separation of the temperature dependent spectra a characteristic temperature, T'_{50G}, is introduced which can be employed as a measure for the temperature dependence of the chain end association in these telechelic ionomers. In this way it is shown that the mobility of an ionic 2,2,6,6-tetramethylpiperidine-N-oxyl derivative is dramatically restricted when compared to the corresponding nonionic probe. For PI the reduction in probe mobility corresponds to temperature shifts as high as 140 K relative to the dynamics of the polymer, indicating the presence of highly immobilized ion multiplets. As shown by the temperature dependent data, the method is sensitive to additional immobilization of the ionic domains induced by bulky substituents adjacent to the ionic chain ends. Comparison of the EPR results with structural data from SAXS measurements reveals that the main factors governing the dynamics of multiplets are the chemical type of ionic end group and the nature of the polymer backbone. Analysis of the EPR data for telechelic PS shows that in high-T_g polymers the dynamics of the ionic aggregates occurs at comparable time scales as the dynamics of the polymer backbone.

Introduction

Self-assembly of molecular systems is a common feature in nature. Microdomain formation as found in block copolymers, colloids, or membranes can be viewed in terms of different effective intermolecular compatibility. In ionomers, *i.e.* polymers containing only a few ionic groups, self-assembly is induced by the incompatibility of ionic and nonionic moieties.[1] The unique properties of these materials are therefore attributed to the existence of ionic aggregates dispersed in a rather unpolar matrix. Since the pioneering work of Eisenberg,[2] there has been a considerable amount of experimental and theoretical work on ionomers as reviewed by Schlick.[3]

Recently, we described the synthesis and characterization of α,ω-macrozwitterionic block copolymers of styrene and isoprene.[4] In these systems, by combining ionic chain end aggregation and microphase separation of block copolymers, the competition between two *distinct* self-assembly processes can be studied. Since the degree of chain end association is crucial for understanding the properties of such ionomeric materials, it is important to find suitable experimental tools for probing the dynamics of these aggregates. In previous work on homopolymers, the impact of counterions on the properties of telechelics was studied thoroughly using differential scanning calorimetry,[5] small angle X-ray scattering,[6] and rheology.[7] It was found for instance that the activation energy for the thermoreversible dissociation of ionic aggregates in α,ω-dicarboxylatopolybutadienes decreases with increasing ionic radius of the cation.[8]

A general model for the phase behavior of ionomers was presented by Eisenberg in which the restricted mobility of polymer segments surrounding so-called multiplets gives rise to a separate high-temperature glass transition above a critical ion content.[9] Experimental support for the restricted mobility of chain segments adjacent to ion multiplets was found by dielectric relaxation using telechelic polyisoprene (PI),[10] NMR using partially deuterated telechelic polystyrene (PS),[11,12] and electron paramagnetic resonance (EPR) by investigating random ionomers with a separate high temperature T_g.[13] In all these studies a significant restriction in chain mobility of polymer segments in the vicinity of ion aggregates, which are on the order of a few nanometers in size, was found. Thus, while most work has focused on the change of polymer properties as a result of ion aggregates,[14,15] little attention has been devoted so far to the description of the multiplets themselves.[16,17] In particular, it is not well-known how the dynamics of ionic domains depend on the chemical type of ionic end group and the nature of the polymer backbone. This is somewhat surprising since e.g. the mechanical properties of ionomers are expected to depend on the dynamics of these nanodomains. Only a few data are available, such as fluorescence[18,19]and NMR studies,[20] on ion pair interchange processes.

In the present work we employ EPR spectroscopy as a tool for studying the dynamics of ion aggregates in monofunctional and α,ω-macrozwitterionic PS and PI homopolymers with sulfonate and ammonium end groups. They serve as model compounds for future investigations of our α,ω-macrozwitterionic block copolymers.[4] The information about dynamics, reflected by the extrema separation in the CW-EPR spectra as a function of temperature, can be used to obtain a rather *general* measure for the temperature dependence of chain end association in telechelic ionomers. Due to the sensitivity of EPR, it is possible to obtain dynamic informations about aggregates in ionomer systems in which the ion content is as low as 0.1%. Consequently, this spectroscopic method can be applied to a large variety of ionomers.

Experimental Section

Polymer Synthesis and Characterization. The monofunctional and α,ω-macrozwitterionic PS and PI homopolymers used in this study are sketched in Figure 1a together with their code names used below. The ionic chain ends were introduced

---

* Author to whom correspondance should be addressed.

⊗ Abstract published in *Advance ACS Abstracts,* May 15, 1997.

S0024-9297(96)01591-4 CCC: $14.00

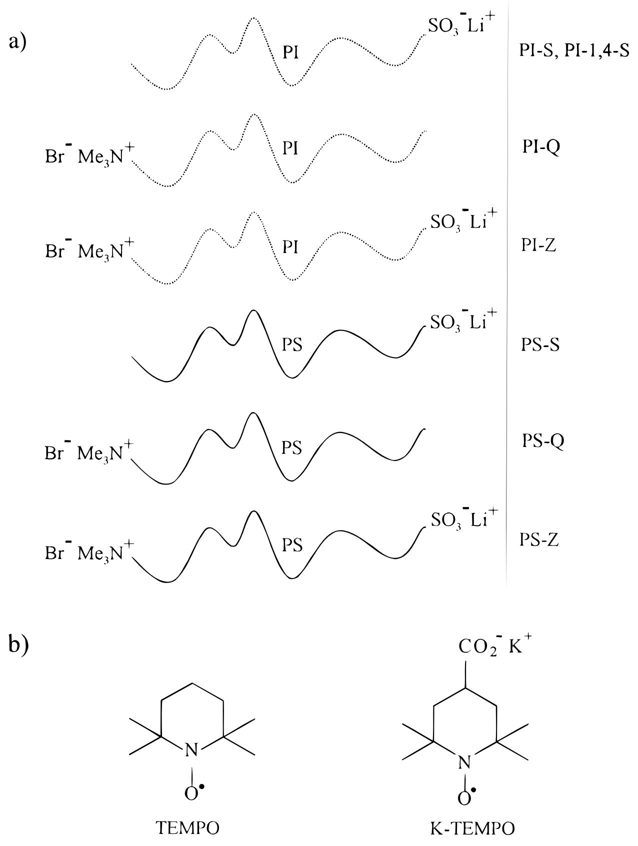

Figure 1. Schematic representation of the telechelic polymers (a) and the chemical structure of the nitroxyl radicals used as spin probes (b).

Table 1. Molecular Characteristics of the Telechelic Polymers[a]

sample	M_n (g/mol)[b]	M_w/M_n[b]	1,4-PI content (%)[c]
PI-1,4-S	5200	1.05	>98
PI-Q(I)			
PI-S(I)	8200	1.30	19
PI-Z(I)			
PI-Q(II)			
PI-S(II)	10000	1.07	19
PI-Z(II)			
PS-Q-5			
PS-S-5	4800	1.07	
PS-Z-5			
PS-Q-35			
PS-S-35	34700	1.04	
PS-Z-35			

[a] For the varying dispersity of the different PI samples see the Experimental Section. [b] As determined by SEC. [c] As determined by ^{1}H-NMR.

by living anionic polymerization using functional initiating and terminating reagents as described previously.[4] In the case of the amine-capped PI, narrow molecular weight (MW) distributions were only obtained when the initiator [2-[(N,N-dimethylamino)methyl]phenyl]lithium was reacted with 1 equiv of 1,1-diphenylethene (DPE) before adding the isoprene. This could be due to possible aggregation of the initiator in the absence of DPE. A PI with 1,4-microstructure was obtained by initiating with s-BuLi in cyclohexane and terminating successively with 1 equiv of DPE and 1,3-propanesultone as described in ref 4. All end-functionalized polymers were purified by chromatography[21] to ensure quantitative end group functionalization. The molecular characteristics of the telechelic polymers are summarized in Table 1.

MW's and MW distributions were measured by size exclusion chromatography (SEC). The microstructure of the PI units was analyzed by ^{1}H-NMR spectroscopy (Bruker AC 300 instrument) in $CDCl_3$ at room temperature. DSC measurements were carried out with a Mettler compensation calorimeter (DSC-30) using a heating/cooling rate of 10 K/min. Evaluation of the DSC curves was performed with a program from the same company. Results on the glass transition temperature, T_g, of different samples are summarized in Table 2. Note that the T_g of PI-1,4-S is significantly lower than those of the other PI derivatives, as expected from the high 1,4-content.

Table 2. T_g and T'_{50G} of the Telechelic Polymers, As determined by DSC and CW-EPR, Respectively

sample	T_g (K)	T'_{50G} (K)
PI-1,4-S	214	356
PI-Q(I)	272	333
PI-S(I)	277	386
PI-Z(I)	278	358
PI-Q(II)	271	352
PI-S(II)	281	379
PI-Z(II)	280	381
PS-Q-5	374	393
PS-S-5	378	433
PS-Z-5	380	387
PS-Q-35	375	395
PS-S-35	379	417
PS-Z-35	381	386

2,2,6,6-Tetramethylpiperidine-*N*-oxyl (TEMPO) and potassium TEMPO carboxylate (K-TEMPO) were the free radicals used (see Figure 1b). TEMPO was purchased from Aldrich, K-TEMPO was obtained by neutralizing the carboxylic acid 4-carboxy-TEMPO (Aldrich) with methanolic KOH. All samples were prepared by the solvent casting method: 100 mg of the polymer dissolved in 10 mL of toluene were mixed with 0.1 mL of a 0.1% spin probe solution (TEMPO in toluene, K-TEMPO in methanol). After solvent evaporation, the samples were transferred into an EPR tube and annealed under vacuum for 1 week (PI at 50 °C; PS at 130 °C).

Instrumentation. EPR spectra were recorded on a Bruker ESP 300 instrument operating in the X-band (*ca.* 9.45 GHz), equipped with a variable temperature accessory (ER 4111 VT). The modulation amplitude was set to 0.2 G using a calibration with fluoranthrenylantimony hexafluoride. In this work the temperature dependent extreme outer peak separation is termed $2\tilde{A}_{zz}$, in order to avoid confusion with the tensor component in the rigid limit 2 A_{zz}; see below.[22]

SAXS measurements were performed with a Kratky compact camera (Anton Paar KG) equipped with a one-dimensional position-sensitive detector (M. Braun). The Ni-filtered Cu Kα radiation ($\lambda = 0.154$ nm) was used from a Siemens generator (Kristalloflex 710 H) operating at 35 kV and 30 mA. The samples were kept in the camera under vacuum in a special brass furnace at room temperature (sample thickness 1 mm). The data were collected in a multichannel analyzer and transferred to a VAX station for further analysis. Smeared intensity data were corrected for absorption, background scattering, and slit-length smearing following the Strobl procedure.[23] Intensities in absolute units were determined by using the moving slit method.

Results and Discussion

1. EPR Spectra of Ionic and Nonionic Probes in Telechelic Polymers.

Before presenting the temperature dependent data of different end functionalized polymers, some general features of nitroxide EPR spectra[22] will be discussed briefly using a PI, end-capped with the lithium sulfonate group and showing 1,4-microstructure (PI-1,4-S). The room temperature EPR spectra of PI-1,4-S doped with TEMPO and K-TEMPO are depicted in Figure 2, parts a and b, respectively. This temperature is about 80 K above the T_g of the polymer (see Table 2).

The TEMPO spectrum of Figure 2a exhibits a characteristic three-line pattern due to the hyperfine splitting with ^{14}N with an outer extrema separation $2\tilde{A}_{zz} \cong$ 35 G. Here, the probe molecules undergo sufficiently

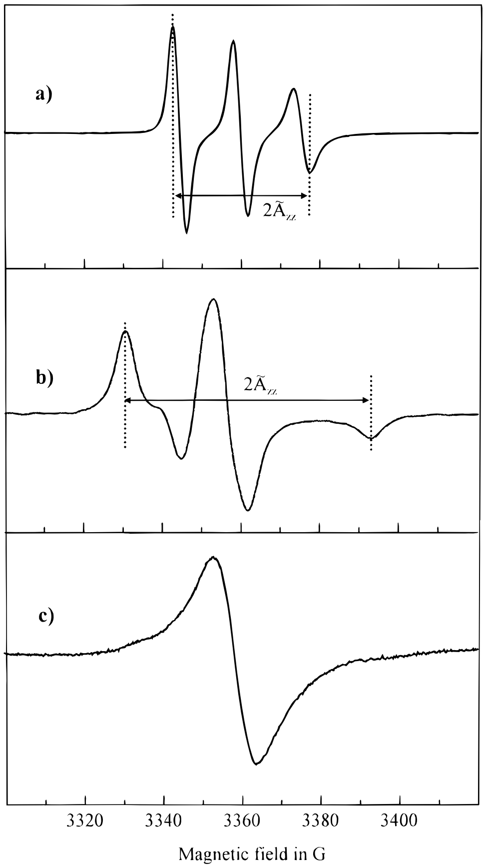

Figure 2. EPR spectra of PI-1,4-S doped with TEMPO (a) and K-TEMPO (b) at room temperature; for comparison: EPR spectrum of *non*functionalized 1,4-PI doped with K-TEMPO (c).

rapid rotation to average out the anisotropies of the coupling tensors, as expected for spin probes in a polymer matrix far above T_g. The spectrum of K-TEMPO in the same polymer is considerably different. It consists of three broad lines with $2\tilde{A}_{zz} \cong 65$ G, indicating slow tumbling of the radicals (Figure 2b). For probe molecules, such a behavior is usually observed at temperatures below the glass transition, where rotational diffusion of the probes is restricted by their highly viscous environment.[24,25]

Since the solubility of ionic radicals in a material with an highly unpolar backbone is expected to be very small, one has to rule out the possibility that phase separation between the K-TEMPO and the polymer occurs. The case of probe clustering can easily be identified, however, by a broad single Gaussian line in the EPR spectrum which arises from electron spin exchange, along with strong dipolar coupling.[26] Such a spectrum is indeed obtained by dispersing K-TEMPO in *non*functionalized PI with 1,4-microstructure ($M_n = 10\,000$ g/mol), as shown in Figure 2c for comparison. The data in Figure 2b thus clearly demonstrate that telechelic ionomers, despite their low ion content (less than 1 mol % in this case) dissolve ionic radicals via ionic interactions. Comparing parts a and b of Figures 2, however, the bound radical obviously exhibits a dramatic reduction in mobility. This effect will be analyzed quantitatively below. Note that the concentration of the radical salt is chosen such that the number of ionic chain ends remains 1−2 orders of magnitude larger than the number of probes. Thus, the structure of the aggregates should be mostly unaffected by the presence of the low molecular weight salt. This was checked by small angle X-ray scattering (SAXS). Indeed, no significant difference in the SAXS pattern could be observed between pure PI-1,4-S and PI-1,4-S, doped with K-TEMPO, when a stoichiometric ratio of 1 probe per 40 sulfonate chain ends was chosen. Moreover, an average functionality of ca. 15 chain ends per multiplet was estimated from the position of the 'ionomer-peak', assuming a simple hexagonal lattice of multiplets[14] (see below). Thus, with an average of less than 0.4 probe molecules per multiplet, the impact of the radical on the multiplet structure is considered to be very small.

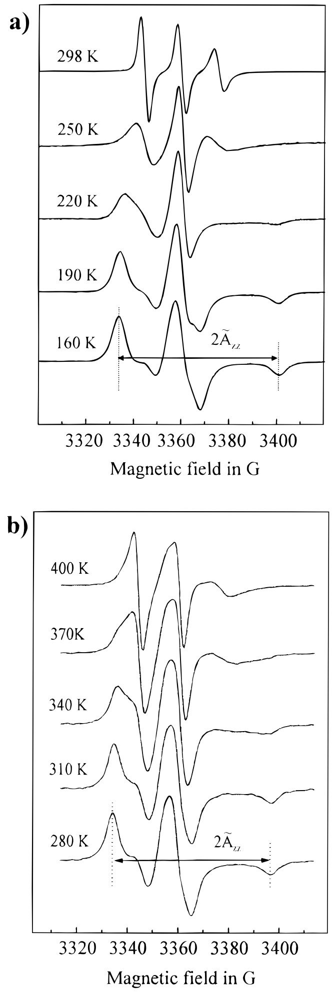

Figure 3. EPR spectra of PI-1,4-S doped with TEMPO (a) and K-TEMPO (b) at different temperatures.

2. Temperature Dependent EPR Spectra. Representative EPR spectra of TEMPO and K-TEMPO in PI-1,4-S measured as a function of temperature are shown in Figure 3, parts a and b, respectively. With increasing temperature, motional narrowing is observed in both cases. The transition from the broad powderlike pattern with $2\tilde{A}_{zz} \cong 65$ G to the motionally narrowed spectrum occurs at much higher temperature for K-TEMPO than for TEMPO; compare the spectra at 190, 220, and 250 K for TEMPO with those for K-TEMPO at 310, 340, and 370 K. CW-EPR is highly sensitive to changes in the rotational correlation time (τ_C) of the probe in the range 10^{-10} s $< \tau_C <$ 10^{-8} s. The line shape in this intermediate regime strongly depends on the frequency *and* the geometry of motion.[27] It should be noted that in the intermediate regime—at temperatures where the extrema separation of the TEMPO and K-TEMPO are comparable (*i.e.* comparable correlation times), e.g. at 220 K for Tempo and 340 K for

K-Tempo—the line shapes significantly differ from each other. This suggests a different geometry of motion in addition to the different temperature dependence: while the almost spherical TEMPO rotates isotropically,[28] the spectra in Figure 3b show evidence for a marked anisotropy in the rotational diffusion of the ionic probe.[29] It may arise from the fact that the K-TEMPO is ionically anchored to ion multiplets. This interpretation is supported by the fact that analogous behavior was recently observed for spin-labels, covalently attached to the chain ends of PS.[29,30] A detailed line shape analysis, however, is beyond the scope of the present study.

In order to compare the mobility of TEMPO and K-TEMPO in PI-1,4-S in a more quantitative way, the values of the extrema separation $2\tilde{A}_{zz}$, are plotted *vs* temperature in Figure 4a. The glass transition of the polymer, as obtained by DSC, is also indicated in the graph. Both curves exhibit a sigmoidal shape with an inflection point at *ca.* 50 G. The temperature at which the outer extrema separation is 50 G has been introduced as T_{50G} in the literature. It is a convenient measure for the mobility of a nitroxide reporter in a specific host matrix.[25] Though being an *indirect* measure for the polymer dynamics, T_{50G} of a specific probe is closely related to the matrix T_g,[31] and a so-called $T_{50G}-T_g$ correlation has been derived theoretically by means of free volume arguments.[32] In the case of PI-1,4-S and TEMPO, T_{50G} is 10 K above the DSC-determined T_g (DSC-T_g), as shown in Figure 4a. In order to confirm the response of the TEMPO to the matrix glass transition of the end functionalized PI, the same probe was incorporated in a *non*functionalized PI of the same microstructure and MW (not shown). In agreement with earlier results[31] and data on natural rubber[33,34] we found the same $T_{50G}-T_g$ proximity for both polymers.

In Figure 4a the inflection point of the ionic probe is shifted by more than 130 K toward higher temperatures when compared to the nonionic TEMPO. It is thus evident that the mobility of the ionic probe must be related to the restricted dynamics of isolated ion multiplets. For motional narrowing in the CW-EPR spectrum of the radical salt to occur, large amplitude thermal motions in the GHz region must overcome mobility restrictions due to Coulombic forces between the charged radical probe and the ionic aggregates. Therefore, in the following, we will use the T_{50G} of K-TEMPO as a measure for the *strength of ion aggregation* of a specific end group in a specific polymer matrix. In order to distinguish between matrix mobility and dynamics of ion aggregates, we term this temperature T'_{50G} (see Figure 4a). We stress at this point that T'_{50G} is a temperature which characterizes the dynamics of the ion aggregates rather than giving a "melting temperature" of the ionic domains.

Note that in the case of PI-1,4-S, T'_{50G} is 142 K above the DSC-T_g. By means of dielectric spectroscopy on a similar telechelic PI it was found that polymer segments in close vicinity of the ion aggregates experience a restriction in mobility corresponding to a temperature shift of only 20−30 K.[10] In related work, for a sulfonated PI, Boiteux *et al.* reported on a high-temperature tan δ maximum ca. 100 K above T_g.[35] Although the authors could not assign this relaxation process, they suggested that it may arise from the thermal dissociation of ion multiplets. Our EPR data clearly show that in these materials softening of ionic bonds (i.e. the onset of dissociation processes) occurs at temperatures *far* above T_g and can be monitored using the spin probe technique. This demonstrates the high sensitivity of EPR to dynamic heterogeneities in these polymers. We will come back to this important point at the end of this paper.

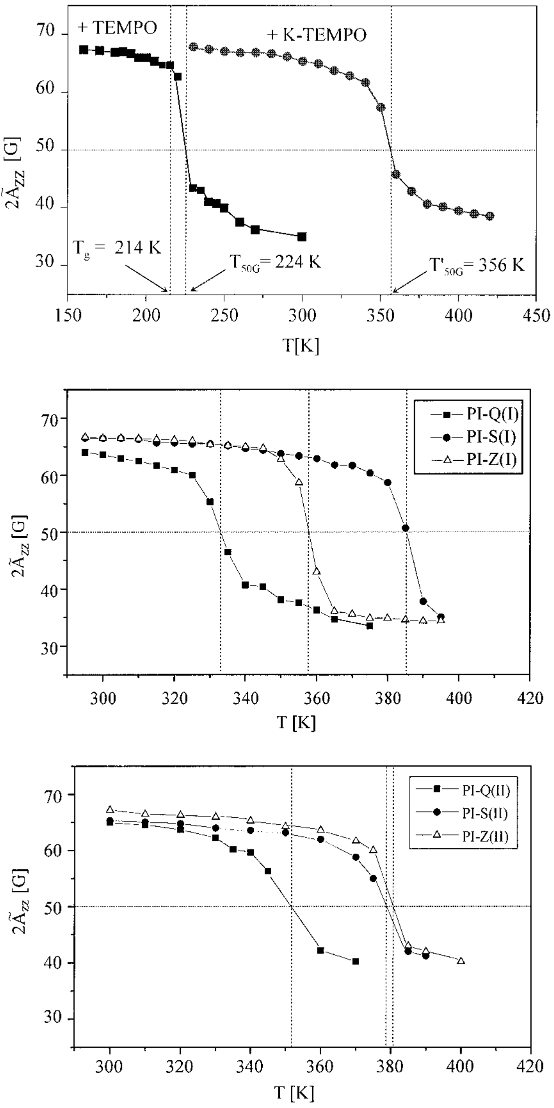

Figure 4. (a) Extreme outer peak separation $2\tilde{A}_{zz}$ *vs* temperature for PI-1,4-S doped with TEMPO (■)and K-TEMPO (●). The lines connecting the data points serve as a guide to the eye. The temperatures at which the outer extrema separation for the two samples is 50 G is indicated by vertical lines. Also indicated by a vertical line is the T_g of the polymer as measured by DSC. (b) Extreme outer peak separation $2\tilde{A}_{zz}$ *vs* temperature for telechelic PI's doped with K-TEMPO. MW's and MW distributions are identical for the ammonium-capped PI-Q(I) (■), the sulfonated PI-S(I) (●), and the macrozwitterionic PI-Z(I) (△) species. The lines connecting the data points serve as a guide to the eye. T'_{50G} of the different samples are indicated by vertical lines. (c) Extreme outer peak separation $2\tilde{A}_{zz}$ *vs* temperature for telechelic PI's doped with K-TEMPO. In contrast to the telechelics in Figure 4b, one DPE unit is placed in between the ammonium group and the PI chain. MW's and MW distributions are identical for the ammonium-capped PI-Q(II) (■), the sulfonated PI-S(II) (●), and the macrozwitterionic PI-Z(II) (△) species. The lines connecting the data points serve as a guide to the eye. T'_{50G} of the different samples are indicated by vertical lines.

3. Comparison of T'_{50G} for Different End Groups. As shown in the previous section, EPR represents a convenient tool which enables detection of the temperature dependence of chain end association in telechelic ionomers. In the following we will employ this technique in order to discriminate between multiplets of different end groups.

3.1. Telechelic PI's. First, telechelic PI's of low 1,4-isoprene content with ammonium bromide (PI-Q(I)), lithium sulfonate (PI-S(I)), and both end groups (PI-Z(I)), as depicted schematically in Figure 1a, are investigated. The molecular characteristics of the three samples are summarized in Table 1. In Figure 4b the values of the extrema separation in the CW spectra, as obtained by mixing the telechelics with K-TEMPO, are plotted against temperature. The T'_{50G} values obtained from the sigmoidal curves are 333, 386, and 358 K for PI-Q(I), PI-S(I), and PI-Z(I), respectively (see Table 2). Thus, the T'_{50G} values cover a range of more than 50 K, whereas the T_gs lie within 6 K. Motional narrowing of the ionic probe occurs 109 K above the DSC-T_g for PI-S(I) but already at 61 K above T_g for PI-Q(I). This observation clearly shows that the mobility of the radical salt significantly depends on the nature of the ionic chain end: The probe is immobilized to a higher extent when attached to lithium sulfonate multiplets compared to ammonium bromide multiplets. Such behavior can be accounted for by considering the difference in dipolar strength: lithium sulfonate, being expectedly a stronger dipole than ammonium bromide, forms multiplets which thermally dissociate at higher temperatures than those of the latter species. It is in agreement with earlier findings that quaternization of an α,ω-(dimethylamino) polymer is responsible for an increase in solution viscosity (toluene, 298 K), although gelation never occurs at higher polymer concentration, in contrast to what happens for the parent metal carboxylate- and sulfonato-telechelic polymers.[36]

In the case of the bifunctional PI-Z(I) the $2\tilde{A}_{zz}$ *vs* T plot shown in Figure 4b yields a T'_{50G} which lies in between the T'_{50G} values of the monofunctional species. The most obvious explanation for this is that ammonium bromide and lithium sulfonate form *mixed* aggregates. The spin probe then reflects an *average* dynamics relative to the pure multiplets. At the same time, T_g, as determined by DSC for all polymers, when compared to the difference in the T'_{50G} values, is rather insensitive with respect to the type of end group (see Table 2). It should be noted that the counterions do participate in the aggregation process. This is supported by the experimental observation that additional amounts of salt can be solubilized by the system. Hence, complete elimination of LiBr from the aggregates can be excluded. It should be emphasized, however, that the specific nature of the ionic interactions within the aggregates is not elucidated in this study. In the following, we will therefore always refer to mixed aggregates in the case of the bifunctional species.

Having established a significant dynamical difference between ammonium bromide and lithium sulfonate aggregates, we now turn to the question if we can even further control the aggregate stability by introducing some bulky "spacers" between the ionic chain end and the polymer chain. This was achieved in a second series of telechelic PI's in which *one* DPE unit is introduced in between the PI-chain and the ammonium group (see experimental part). Their code names are PI-Q(II), PI-S(II), and PI-Z(II); see Table 1. The $2\tilde{A}_{zz}$ *vs* T plots as obtained from the temperature dependent spectra are shown in Figure 4c. The T'_{50G} values of the three samples are 352, 379, and 381 K for PI-Q(II), PI-S(II), and PI-Z(II), respectively, as summarized in Table 2. As expected, T'_{50G} of PI-S(II) is almost identical with that of PI-S(I), since the DPE at the ammonium should not affect ionic aggregation of the sulfonated second chain end. This situation changes when the amine-capped species with DPE next to it is quaternized and now participates in the aggregation process: T'_{50G} of PI-Q(II) is roughly 20 K above the value obtained for PI-Q(I). These data indicate that the mobility of the ionic spin probe is *further* reduced by introducing bulky substituents next to the ionic chain end. It is thereby demonstrated that the present spin probe technique represents a powerful tool which is even sensitive toward small changes in the environment of ion aggregates.

For the bifunctional species PI-Z(II), a different situation is found compared to PI-Z(I): Instead of finding an *average* T'_{50G} for PI-Z(II) [i.e. in between T'_{50G} of PI-Q(II) and PI-S(II)] T'_{50G} almost coincides with T'_{50G} of PI-S(II). Though structural data show evidence for *mixed* aggregates consisting of sulfonate and ammonium groups (see below), the dynamics appear to be rather dominated by the more stable sulfonate groups. Whether this is a result of polydispersity or of more efficient packing of ionic chain ends is unclear at the moment and requires further investigations.

The impact of the glass transition temperature, i.e. the nature of the polymer backbone, upon T'_{50G} is demonstrated by comparing PI-1,4-S with PI-S(I): When T_g is raised from 214 to 277 K, an increase in T'_{50G} from 356 to 386 K is found (see Table 2). Thus, the nature of the polymer backbone also influences the dissociation process of the multiplets. Higher mobility favors dissociation since in a fully relaxed polymer the chain ends tend to adopt a random distribution.

In summary, so far we have identified two factors governing the dynamics of ion multiplets in ionomers: (a) the nature of the ionic chain end (Multiplets composed of strong dipoles dissociate at higher temperatures than multiplets of weak dipoles.) and (b) the T_g of the polymer (The lower T_g of the polymer, the stronger the tendency of the chain ends to dissociate.).

Comparison with SAXS Data. Another factor which should influence the multiplet dynamics is the size of the ionic aggregates. In order to correlate the observed T'_{50G} values for the different end groups with the respective multiplet size, we performed SAXS experiments on these materials. It is well-established that the "ionomer peak" determined by SAXS reflects the average intermultiplet distance[6]. Therefore, by assuming that all chain ends are packed in an hexagonal lattice of multiplets it is possible to estimate an average aggregation number n from the peak position d_{Bragg}[14]

$$n = \frac{10^{-19}\rho N_A f {d_{\mathrm{Bragg}}}^3}{\sqrt{2M_n}} \tag{1}$$

where ρ is the polymer density (g/cm^3), N_A Avogadro's constant, f the end-functionality of the chains, and M_n the number-average molecular weight. SAXS profiles of PI-Q(II), PI-S(II), and PI-Z(II) at room temperature are depicted in Figure 5. In all three cases a peak is obtained in the SAXS profiles. It is strongest for the macrozwitterions PI-Z(II) and weakest for PI-Q(II). The difference in absolute intensities at $q_{\max}$ can qualitatively be attributed to the difference in electron density contrast for the three samples. It is higher for the case of sulfonate end groups than for the case of ammonium ions. The intensity is highest for the bifunctionals PI-

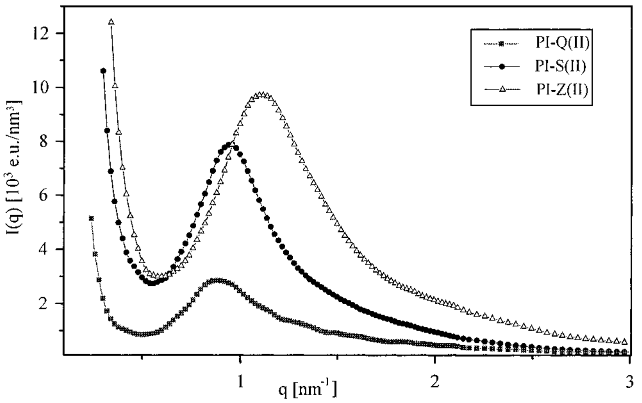

Figure 5. SAXS profiles of PI-Q(II) (■), PI-S(II) (●), and PI-Z(II) (△) at room temperature.

Z(II) since there the charge density is largest. From these data d_{Bragg} was determined as 7.1, 6.7, and 5.7 nm for PI-Q(II), PI-S(II), and PI-Z(II), respectively. From eq 1, the average size of multiplets is estimated to be $n = 13$, 11, and 14 for PI-Q(II), PI-S(II), and PI-Z(II), respectively. The number of chain ends per multiplet is thus slightly *smaller* for the lithium sulfonate groups compared to the ammonium bromides. This is in agreement with earlier findings that in the case of α,ω-alkalino-earth carboxylato polybutadiene, the mean size of the ionic aggregates (multiplets) increases inversely with the ion pair interactions.[8] At first sight this seems counterintuitive, since one would expect larger aggregation numbers for stronger dipoles. Another factor that should be taken into account, however, is the size of the end groups. For steric reasons multiplets consisting of the larger ammonium end groups may accomodate more chain ends than those consisting of the smaller sulfonate groups. Thus, it can be concluded that sulfonate end groups form aggregates in PI which, though being somewhat *smaller* in size, dissociate at higher temperatures than those formed by ammonium end groups. This emphasizes the importance of the chemical nature of the ionic end group in determining the dynamics of the ion multiplets.

3.2. Telechelic PS's. The applicability of the presented EPR spin probe technique to other ion-containing polymer systems was investigated by studying the dynamics of ion aggregates in various end functionalized PS samples, as shown schematically in Figure 1a. The molecular characteristics of these telechelics are listed in Table 1 together with their code names. PS is an interesting case since its T_g of about 380 K is in the range of temperatures, where the onset of mobility of the ionic aggregates was observed for PI, as reflected in the T'_{50G} values; see above. The extrema separation of PS-S-5, PS-Q-5, and PS-Z-5, as obtained from temperature dependent EPR spectra using K-TEMPO as the probe, are plotted in Figure 6. The T'_{50G} values determined from these plots are 433, 387, and 393 K, respectively. Note, that only in the case of PS-S-5, the T'_{50G} value (433 K) is significantly above the DSC-T_g, while in the case of PS-Q-5 and PS-Z-5, T'_{50G} (387 and 393 K) is indeed found to be very close to the DSC glass transition temperature. This contrasts with the telechelic PI's discussed above, for which all T'_{50G} values were well above the DSC-T_g (see the next paragraph). The higher T'_{50G} found for PS-S-5, again demonstrates that the probe is immobilized to a higher extent when attached to lithium sulfonate than to ammonium bromide groups. The same behavior was reproduced for telechelic PS of much higher MW (see Table 2).

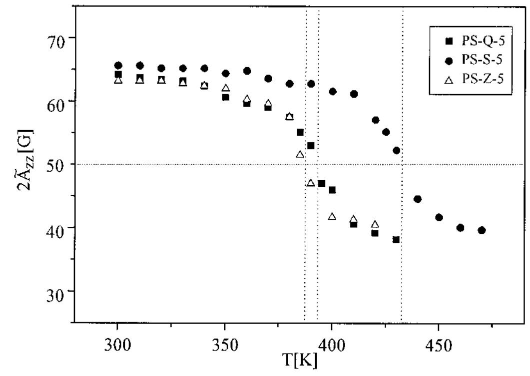

Figure 6. Extreme outer peak separation $2\tilde{A}_{zz}$ *vs* temperature for telechelic PS's doped with K-TEMPO. MW's and MW distributions are identical for the ammonium-capped PS-Q-5 (■), the sulfonated PS-S-5 (●), and the macrozwitterionic PS-Z-5 (△) species. T'_{50G} of the different samples are indicated by vertical lines.

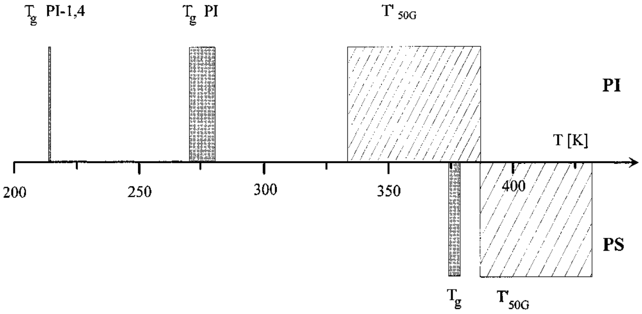

Figure 7. Schematic representation of T_g (gray areas) and T'_{50G} (hatched areas) values for the different PI (upper side) and PS (lower side) samples used in the present study. The drastic difference between T_g and T'_{50G} values for PI can only be explained by the existence of ion multiplets with strong mobility restrictions. The close vicinity of T_g and T'_{50G} values for PS makes interpretation of the effects ambiguous as described in the text.

3.3. Comparison of Ionic and Nonionic Chain End Dynamics. In order to illustrate the difference in mobility for ionic and nonionic domains as evidenced by the present spin probe technique, T_g and T'_{50G} values for all polymers studied in this work are schematically depicted in Figure 7. A marked difference between the PS and PI samples clearly shows up: While for all PI samples T'_{50G} is found *far* above T_g, the T'_{50G} values of the PS's are close to the glass transition. In previous studies performed in our group,[29] for PS *end-labeled* with a TEMPO molecule $T_{50G} = 423$ K was determined. Comparing this temperature with the T'_{50G} regime of PS shown in Figure 7 (hatched area lower side), it is clear that for this polymer the dynamics measured by the CW-EPR spectra of K-TEMPO is comparable with the dynamics of the labeled nonionic chain end. Given the "universal" values $c_{1g} = 17.4$ and $c_{2g} = 51.6$ K in the WLF equation,[37] for PI the dynamics of the polymer backbone reaches the gigahertz frequency regime roughly 50 K above T_g, as measured by DSC. T_{50G} of an end-labeled PI polymer sample would thus be at most 50 K above the DSC-T_g. Since the measured values of T'_{50G} are up to 130 K above the DSC-T_g, for this polymer, only the existence of strongly immobilized ion multiplets can account for the behavior of the ionic probe. For PS, however, the CW-EPR spectra of K-TEMPO can also be interpreted on the basis of spin probes sticking to the chain-ends due to dipolar interactions. In a recent work about EPR on PS−PVME blends we have shown that the same shift of T_{50G} with respect to T_g is observed when there are additional interactions between the spin probe and the polymer.[38] From this comparison we conclude that in the case of end functionalized PS it is difficult to decide from CW-EPR data of ionic probes whether motional narrowing occurs because the probe is immobilized at ion multiplets which dissociate *or* because the probe simply behaves as a spin label ionically attached to the chain end. At this point we refer to a recent EPR study on a PS-based random ionomer. Using a similar spin probe the observed reduction in probe mobility was attributed to the presence of ion multiplets.[13] We think that at least for PS-ionomers with low ion-content such a conclusion should not be based on EPR-data alone.

Conclusions

In the present work it is shown that polymers end functionalized with ionic groups can be characterized by EPR using the spin probe technique: When an ionic TEMPO-derivative is dispersed in a telechelic ionomer, the extrema separation of the temperature dependent CW-EPR spectra demonstrate a severe restriction in mobility of the radical. In difference to earlier contributions dealing with ionomer models, with this study we emphasize that the dynamic informations, as obtained by EPR, enable a more detailed description of these aggregates themselves. It is found that the probe dynamics is a sensitive measure for the temperature dependence of chain end association within distinct multiplets. The strength of the chain end association is found to depend markedly on the nature of the polymer backbone, as reflected in the T_g, and the nature of the ionic end group. The sensitivity of the present technique is further demonstrated by a high temperature shift caused by bulky substituents adjacent to the ionic chain ends. When compared to the results of earlier dielectric and NMR spectroscopic investigations,[10,11] the dynamic contrast between ionic and nonionic domains, detected by EPR, is much more pronounced. Moreover, whereas these measurements were restricted to low molecular weight or isotope-labeled chains, the present EPR-spin-probe technique is applicable to a large variety of polymer samples due to the high sensitivity of this spectroscopic method. In the case of high-T_g materials, the dynamics of the ion aggregates become comparable with the dynamics of the polymer backbone, as demonstrated for ionically end-capped PS samples. In summary, the spin probe technique can serve as a convenient tool to characterize ion aggregation in ionomers, and further studies on end functionalized block copolymers are now in progress in our laboratory.

Acknowledgment. The financial support by the Deutsche Forschungsgemeinschaft, Schwerpunkt Polyelektrolyte, and a scholarship (V.S.) provided by the Studienstiftung des deutschen Volkes is gratefully acknowledged. Also, we would like to thank the Polymer-Analytik division of our institute for their collaboration, the EPR-group for technical assistance with the CW spectrometer, and Ute Pawelzik for the DSC measurements.

References and Notes

(1) Pineri, M.; Eisenberg, A. (Eds.) *Structure and Properties of Ionomers*, NATO ASI Series 198; D. Reidel Publ. Co.: Dordrecht, Holland, 1987.

(2) Eisenberg, A. *Macromolecules* **1970**, *3*, 147.

(3) Schlick, S. *Ionomers, Characterizaion, Theory, and Applications*; CRC Press, New York, 1996.

(4) Schädler, V; Spickermann, J.; Räder, H.-J.; Wiesner, U. *Macromolecules* **1996**, *29*, 4685.

(5) Jérôme, R.; Horrion, J.; Fayt, R.; Teyssié, P. *Macromolecules* **1984**, *17*, 2447.

(6) Williams, C. E.; Russell, T. P.; Jérôme, R.; Horrion, J. *Macromolecules* **1986**, *19*, 2877.

(7) Broze, G.; Jérôme, R.; Teyssié; P., Marco, C. *J. Polym. Sci. Polym. Lett. Ed.* **1983**, *21*, 2205.

(8) Jérôme, R. Halato-Telechelic Polymers: A New Class of Ionomers. In: *Telechelic Polymers: Synthesis and Characterization*; CRC Press: FL, 1989.

(9) Eisenberg, A.; Hird, B.; Moore, R. B. *Macromolecules* **1990**, *23*, 4098.

(10) Yano, S.; Tadano, K.; Jérôme, R. *Macromolecules* **1991**, *24*, 6439.

(11) Vanhoorne, P.; Jérôme, R.; Teyssié, P.; Lauprêtre, F. *Macromolecules* **1994**, *27*, 2548.

(12) Gao, Z.; Xing-Fu, Z.; Eisenberg, A. *Macromolecules* **1994**, *27*, 794.

(13) Tsagaropoulos, G.; Kim, J.-S.; Eisenberg, A. *Macromolecules* **1996**, *29*, 2222

(14) Vanhoorne, P.; Jérôme, R. Contribution of Halato-Telechelic Polymers to the Modellization of Morphology and Solution Properties of Ionomers in ref. 3, p 187.

(15) Kim, J.-S.; Eisenberg, A. Ion Aggregation and its Effects on Ionomer Properties in ref 3, p 7.

(16) Semenov, A. N.; Nyrkova, I. A.; Khokhlov, A. R. *Macromolecules* **1995**, *28*, 7491.

(17) Broze, G.; Jérôme, R.; Teyssié, P.; Gallot, B. *J. Polym. Sci., Polym. Lett. Ed.* **1981**, *19*, 415.

(18) Morawetz, H.; Wang, Y. *Macromolecules* **1988**, *21*, 107.

(19) Dowling, K. C.; Thomas, J. K. *Macromolecules* **1991**, *24*, 4131.

(20) Vanhoorne; P.; Grandjean, J.; Jérôme, R. *Macromolecules* **1995**, *28*, 3553.

(21) Antonietti, M.; Heyne, J.; Sillescu, H. *Makromol. Chem.* **1991**, *192*, 3021.

(22) Cameron, G. G. *ESR Spectroscopy* in *Polymer Characterization*, Booth, C., Price, C., Eds. London, 1987; Vol. 1, Chapter 23, p 517.

(23) Strobl, G. R. *Acta Crystallogr.* **1970**, *A26*, 367.

(24) Rozantsev, E. G. *Free Nitroxide Radicals*; Plenum, New York, 1970.

(25) Rabold, G. P., *J. Polym. Sci*., A-1, **1969**, *7*, 1203.

(26) Wertz, J. E.; Bolton, J. R. *Electron Spin Resonance*; London, 1986; pp 197−203.

(27) Freed, J. H. Theory of Slow Tumbling ESR Spectra for Nitroxides. In: Spin Labelling; Berliner, L. J., Ed.; Academic Press: London, 1976.

(28) Tormälä, P.; Weber, G.; Lindberg, J. J. Spin Label and Probe Studies of Relaxations and Phase Transitions in Polymeric Solids and Melts. Boyer, R. F., Keinath, S. E., Eds.; *Molecular Motion in Polymers by ESR*; Harwood Academic Publishers: New York, 1978

(29) Volkmer, T.; Wiesner, U.; Brombacher, L. Spiess, H. W., *Macromol. Chem. Phys.* **1996** *197*, 1121.

(30) Saalmüller, J. W.; Long, H. W.; Volkmer, T.; Wiesner, U.; Maresch, G. G.; Spiess, H. W. *J. Pol. Sci. B* **1996**, *34*, 1093.

(31) Kumler, P. L.; Boyer, R. F. *Macromolecules* **1976**, *9*, 903.

(32) Bullock, A. T.; Cameron, G. G.; Miles, I. S. *Polymer* **1976**, *23*, 1536.

(33) Kovarskii, A. L.; Vasserman, A. M.; Buchachenko, A. L. *Vysokomol. Soedin. A*, **1971**, *13*, 1647.

(34) Weber, G.; Törrmälä, P. *Colloid Polym. Sci.* **1978**, *256*, 638.

(35) Boiteux, G.; Foucart, M.; Jérôme, R. *Polymer* **1992**, *33*, 4242.

(36) Charlier, P.; Jérôme, R.; Teyssié, P. *Polymer* **1993**, *34*, 369.

(37) Ferry, J.-D., *Viscoelastic Properties of Polymers*; Wiley: New York, 1980.

(38) Volkmer, T.; Pinhal, N.; Hubrich, M.; Sammet, A.; Spiegel,S.; Wiesner, U.; Spiess, H. W. Manuscript in preparation.

MA961591+